Bismuth-Functionalized Silica Aerogels for Iodine Capture

Nuclear Technology Research & Development

Prepared for
U.S. Department of Energy
J. Matyáš, E.S. Ilton, N. Lahiri, X.S. Li, and J.A. Silverstein
Pacific Northwest National Laboratory
September 30, 2021
PNNL-32086

SUMMARY

The U.S. Department of Energy is looking into alternative sorbents for the removal of radioiodine from off-gas streams in a used nuclear fuel reprocessing plant. One class of sorbents considered are bismuth-functionalized silica aerogels, which offer an efficient capture of iodine from off-gas streams and are environmentally friendly as well as lower cost alternatives compared to silver-functionalized sorbents.

Two types of bismuth-functionalized silica aerogels were successfully manufactured using a hierarchical synthesis approach including Bi^{3+}-aerogels with bismuth oxide nitrate hydroxide hydrate particles and Bi-aerogels with bismuth metal and bismuth sulfide nanoparticles. Both sorbents exhibited high sorption capacity for iodine. However, the presence of particles of different composition, size, and distribution on aerogel supports resulted in different iodine loadings. The Bi^{3+}-aerogel exhibited sorption capacity of 289 mg/g. In contrast, Bi-aerogels exhibited more than 20% higher sorption capacity. The heat-treatment of Bi^{3+}-aerogel at 225°C under hydrogen atmosphere increased iodine loading capacity to 351 mg/g.

CONTENTS

FIGURES

ABBREVIATIONS

ads/des	adsorption/desorption
Ag^0-aerogel	silver-functionalized silica aerogel
Ag^+-aerogel	silver ion impregnated silica aerogel
$AgNO_3$	silver nitrate
Ag^0Z	silver mordenite
BET	Brunauer–Emmett–Teller
Bi^{3+}-aerogel	bismuth impregnated silica aerogel
Bi-aerogel	bismuth aerogel
BJH	Barrett–Joyner–Halenda
CH_3OH	methanol
FWHM	full width at half maximum
INL	Idaho National Laboratory
ORNL	Oak Ridge National Laboratory
PE	pass energy
S	specific surface area
SEM-EDS	scanning electron microscopy and energy dispersive spectroscopy
V	pore volume
XPS	X-ray photoelectron spectroscopy
XRD	X-ray diffraction analysis

1 INTRODUCTION

Silver-functionalized silica aerogel (Ag^0-aerogel) was successfully developed for the removal and sequestration of iodine compounds from the off-gas of a nuclear fuel reprocessing plant (Matyáš et al. 2011). Numerous laboratory and bench scale tests of this sorbent in simulated dissolver off-gas gas streams demonstrated iodine capacities of up to 480 mg/g with decontamination factors over 10,000 (Matyáš et al. 2011; Soelberg and Watson 2012), high selectivity and sorption capacity for iodine even after a long-term exposure to oxidizing off-gas streams at 150°C (Bruffey et al. 2012, 2013; Jubin et al. 2014; Bruffey et al. 2015a; Bruffey et al. 2015b), improved mechanical properties (Matyáš et al. 2018; Matyáš et al. 2020) and stability in aggressive oxidizing off gas streams over silver mordenite (Ag^0Z), more than six to eleven times higher sorption capacity than the Ag^0Z (Matyáš et al. 2020; Tavlarides 2019), and promising sorption performance in the presence of other halogens (Matyáš et al. 2021).

The main purpose of this exploratory study was to develop bismuth-functionalized silica aerogels (BFSAs). Bismuth functionalization of environmental sorbents is considered an attractive option to replace silver as an active ingredient for iodine capture from reprocessing off-gas streams. The driver for this change comes from lower cost and environmentally benign character of bismuth. An array of experimental tools was used to synthesize, characterize and test BFSAs. The changes in the microstructure and porosity were followed with the Brunauer–Emmett–Teller (BET) analysis. Scanning electron microscopy and energy dispersive spectroscopy (SEM-EDS) was employed to visualize morphology, size, and distribution of particles on silica aerogel support. X-ray photoelectron spectroscopy (XPS) was used to explore the chemistry at the surface of the samples and X-ray diffraction analysis (XRD) was used identify crystalline phases present in samples. Static iodine sorption testing was used to evaluate sorption performance of developed bismuth-functionalized aerogels.

2 MATERIAL

In this study, BFSAs were prepared, characterized, and evaluated for their iodine sorption capacities. First, thiol-modified aerogel (SH-aerogel) was synthesized from commercially available silica aerogel granules (>2 mm, United Nuclear, Laingsburg, MI). These granules were impregnated with bismuth nitrate solution to prepare Bi^{3+}-aerogel, which was then heat-treated at 225°C under hydrogen to manufacture Bi-aerogel.

Granules of silica aerogel were heated from room temperature to 725°C at a rate of 5°C/min to remove trimethylsilyl groups installed by the manufacturer to make the aerogel hydrophobic, and then hydrated in humidity-saturated air for ~24 h. Following hydration, 3-(mercaptopropyl)trimethoxysilane [$HS(CH_2)_3Si(OCH_3)_3$, 95%] (Sigma Aldrich, St. Louis, MO) was distributed throughout the granules using a syringe at ~2 mL per g of unhydrated sample. The wetted material was loaded into a 1 L high-pressure vessel that was then heated to 150°C, the vessel was filled with supercritical CO_2 at 24 MPa, and the sample cooked for 7 days to produce SH-aerogel. Following this process, the SH-aerogels (~3 g, white granules) were altered by installing the Bi^{3+} ions through a 2-hr treatment with 75 mL of bismuth nitrate solution. This solution was prepared by dissolving 7 g of bismuth nitrate pentahydrate [$Bi(NO_3)_3 \cdot 5H_2O$, ≥98%, Sigma Aldrich] in 100 mL of acetone. The clear bismuth solution was obtained by filtering out the white precipitate of bismuth oxynitrate with a 0.2 µm filter. After impregnation with bismuth was completed, the yellow granules of Bi^{3+}-aerogel were separated from solution and dried in the fume hood for 24 h. The Bi-aerogels (dark brown granules) were produced from Bi^{3+}-aerogel by treatment under 100% hydrogen by heating at 1°C/min from room temperature to 225°C, holding there for 4 h, and cooling down at 5°C/min from 225°C to room temperature.

3 EXPERIMENTAL METHODS OF INVESTIGATION

The BET analysis was utilized to investigate changes in the microstructure and porosity. The scanning electron microscopy and energy dispersive spectroscopy (SEM-EDS) was employed to investigate

morphology and phase distribution. The X-ray photoelectron spectroscopy (XPS) was used to explore the chemistry at the surface of the samples. The X-ray diffraction analysis (XRD) helped identify crystalline phases present in samples. Static iodine sorption testing was used to determine iodine loading capacities.

3.1 Brunauer–Emmett–Teller analysis

The BET analysis was performed on samples degassed at 25°C under vacuum. The data from nitrogen adsorption/desorption (ads/des) at 77 K were collected with an Autosorb 6-B gas sorption system (Quantachrome Instruments, Boynton Beach, FL). The surface area was determined from the isotherm using the five-point BET method. The Barrett–Joyner–Halenda (BJH) method was used to calculate the pore volume and average pore size.

3.2 Scanning electron microscopy and energy dispersive spectroscopy

Bismuth-functionalized silica aerogels in the form of granules and powder were secured to carbon tape and characterized with a JSM-7001F/TTLS (JEOL Ltd., Tokyo, Japan) SEM. The SEM is equipped with a field emission gun and capable of examining specimens under variable pressure conditions, allowing them to be evaluated without a conductive coating and under a low vacuum.

3.3 X-ray photoelectron spectroscopy

Bismuth-functionalized silica aerogels were analyzed with Kratos AXIS Ultra DLD XPS system equipped with a hemispherical analyzer using a monochromatic Al-Ka source ($h\nu$ = 1486.7 eV) operated at 150 W. The samples were transferred into an argon glovebox (O_2 < 0.5 ppm and H_2O < 0.2 ppm) and crushed using a mortar and pestle. The powder was secured onto double sided tape and samples moved into the fast entry port of the instrument attached to the glovebox. Analysis was performed at a chamber pressure of $<2\times10^{-9}$ Torr without ion-sputtering. Sample surface charging was minimized using a low-energy electron flood gun. Data was acquired on an area of 700 mm × 300 mm at a normal take-off angle. Survey scans were acquired at a pass energy (PE) of 160 eV and a step size of 1 eV, while high-resolution scans were acquired at a PE of 40 eV and a smaller step size of 0.1 eV. A sputter cleaned Au foil yielded a full width at half maximum (FWHM) of 1.9 eV when using a PE of 160 eV, while a PE of 40 eV yields a FWHM of 0.8 eV. The data were processed using CasaXPS software and charge referenced to the C 1s (C-C/C-H component) at 285 eV. An iterative Shirley background was used for the dataset. The peaks were fitted using Gaussian-Lorentzian type curves.

3.4 X-ray diffraction analysis

Selected samples were ground with an agate mortar and pestle, suspended in a few drops of ethanol, dropwise deposited onto a 25-mm zero-background silicon holder, dried, and analyzed with a D8 Advance (Bruker AXS Inc., Madison, WI) XRD with Cu Kα emission. The instrument was equipped with a LynxEye position-sensitive detector with a collection window of 3° 2θ. Scan parameters were 5−80° 2θ with a step of 0.009° 2θ and a 2-s dwell at each step. Bruker AXS DIFFRAC^{plus} EVA (v14) was used to identify the crystalline phases.

3.5 Static sorption test

A Teflon® assembly, which consisted top and bottom vessels connected by two vertical tubes, was used for iodine sorption capacity measurements under static conditions (Matyáš et al. 2019). The top vessel contained six glass vials, each with ~150 mg of granules. The bottom vessel encompassed ~0.6 g of solid iodine. The assembly was kept in an oven at 150°C for 24 h. To remove loosely bonded or excess iodine from the samples following sorption, the vials were transferred into a desiccator (10 kPa in-house

vacuum) for 24 h. Subsequently, the sorbent was removed and weighed on an analytical balance of 0.1 mg sensitivity to obtain the iodine sorption capacities.

4 RESULTS

Produced SH-aerogel exhibited specific surface area (S) of 184 m^2/g, pore volume (V) of 1.4×10^{-6} m^3/g, and adsorption/desorption (ads/des) pore size of 33/24 nm, respectively. This indicates a high degree of pore surface functionalization with propylthiol monolayer when compared to raw silica aerogel (S = 1100 m^2/g, $V = 8.1\times10^{-6}$ m^3/g, and ads/des = 57/19 nm). A high degree of thiolation provided a chemical foundation for an efficient room temperature functionalization with bismuth. The produced Bi^{3+}-aerogels exhibited S = 151 m^2/g, $V = 0.77\times10^{-6}$ m^3/g, ads/des = 32/19 nm, respectively. Additional changes were observed after its treatment under hydrogen flow. The synthesized Bi-aerogel showed S = 196 m^2/g, $V = 0.93\times10^{-6}$ m^3/g, ads/des = 32/19 nm, respectively. The increase in S and V, when compared to Bi^{3+}-aerogel, can be attributed to formation of small nanoparticles on the pore walls and some structural modification of propylthiol monolayer chemistry.

Figure 1, Figure 2, and Figure 3 show XRD patterns with identified phases for Bi^{3+}-aerogel, Bi-aerogel, and iodine-loaded Bi-aerogel. The only crystalline phase identified in Bi^{3+}-aerogel was bismuth oxide nitrate hydroxide hydrate [$Bi_6O_5(OH)_3(NO_3)_5\cdot2H_2O$]. This phase precipitated from clean bismuth nitrate solution during impregnation of SH-aerogel. The heat-treatment of Bi^{3+}-aerogel in hydrogen produced Bi-aerogel with nanoparticles of bismuth metal and bismuth sulfide. An exposure of Bi-aerogels to iodine gas produced BiI_3. There were no other crystalline phases present.

Figure 4 shows the morphology and distribution of bismuth oxide nitrate hydroxide hydrate nanoparticles on the surface of the granule for Bi^{3+}-aerogel. A high number of particles formed with a tendency to agglomerate into bigger clusters. This landscape of particles got rearranged significantly after heat-treatment in hydrogen. Figure 5 shows nanoparticles of bismuth and bismuth sulfide on the surface of Bi-aerogels. The nanoparticles were about the same size (~50 nm) and uniformly distributed on the surface of the silica aerogel support. Another change in morphology and size of particles occurred after the sorption test. These nanoparticles got converted into 10-µm hexagonal plates of BiI_3 after a day-long exposure to iodine vapors. Figure 6 shows an SEM micrograph of BiI_3 crystals for iodine-loaded Bi-aerogel compared with overlay EDS dot maps for Bi and I.

For XPS of Bi^{3+}-aerogel, shown in Figure 7, the binding energy (BE) of Bi $4f_{7/2}$ for pre-crushed and freshly crushed granules occurs at 159.3-4 and 160.3-4 eV, indicating two different species of Bi but both forming Bi-O bonds. The higher BE species may indicate Bi-O-C bonds whereas the more dominant lower BE species suggest Bi oxide that could correspond to $Bi_6O_5(OH)_3(NO_3)_5\cdot2H_2O$ identified by XRD. The freshly crushed sample (i.e., exposing more of the virgin interior of the aerogel) contained a higher proportion of the species at 160. 3 eV. The S2s binding energy is consistent with thiol. Consequently, there is no evidence for Bi-thiol bonds or Bi_2S_3. For Bi-aerogel, shown in Figure 8, the BE of Bi $4f_{72}$ decreased to 158.8-9 eV for the dominant species and some thiol was reduced to sulfide. Both observations are consistent with the formation of Bi_2S_3 as indicated by XRD analyses. However, the amount of sulfide is not sufficient to account for all the Bi. Interestingly, XRD also shows the presence of Bi metal. This is curious as the BE of Bi^0 is nominally around 156-157 eV (for bulk metal), which was not detected by XPS. In this regard, we note that XRD shows very broad peaks for Bi^0, indicating nanoscale particles. Hence, we speculate that the $4f_{7/2}$ BE of Bi^0 might increase with decreasing particle size, akin to the behavior of silver metal, and possibly overlap the BE of Bi_2S_3. This hypothesis warrants further work.

The iodine sorption capacity for Bi^{3+}-aerogel, as determined from static sorption test, was 289 mg of I_2 per g of sorbent. However, Bi-aerogel exhibited more than 20% higher sorption capacity. The treatment of Bi^{3+}-aerogel in hydrogen increased iodine loading capacity to 351 mg/g. This difference demonstrates that iodine sorption is significantly affected by bismuth chemistry and its oxidation state.

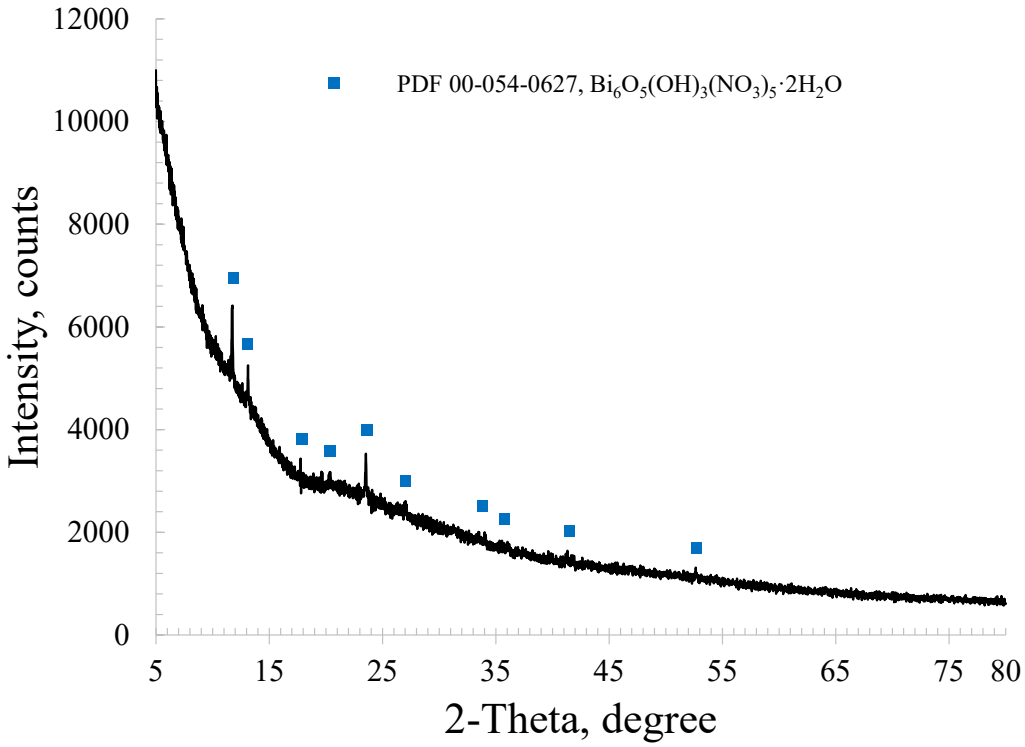

Figure 1. XRD pattern with identified phase for Bi^{3+}-aerogel.

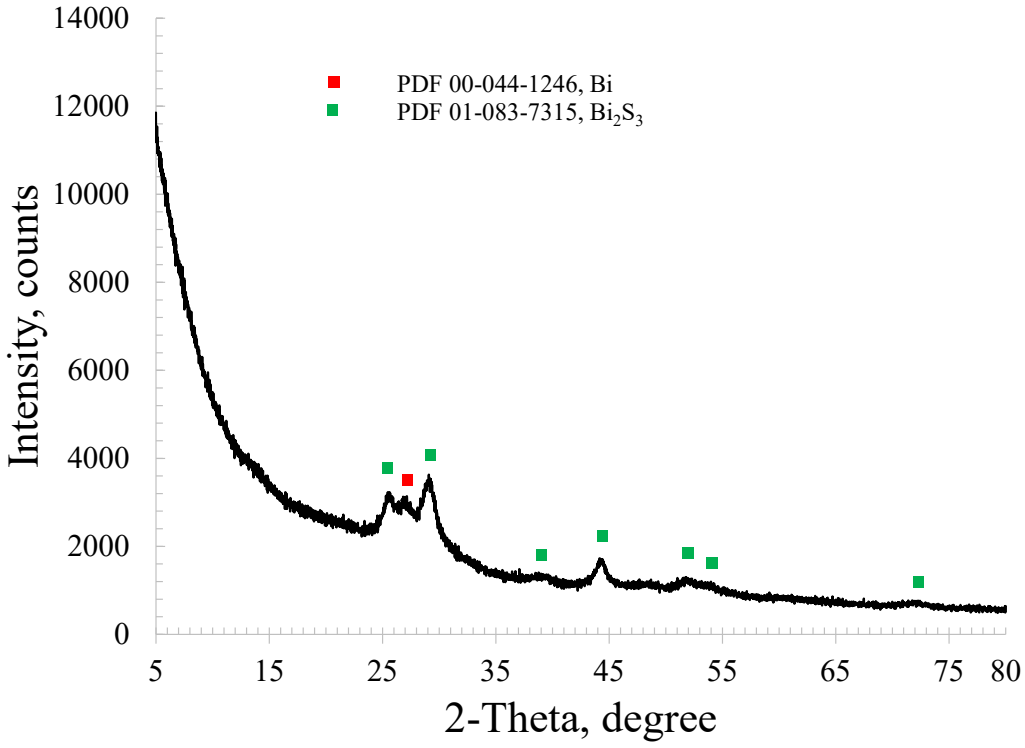

Figure 2. XRD pattern with identified phases for Bi-aerogel.

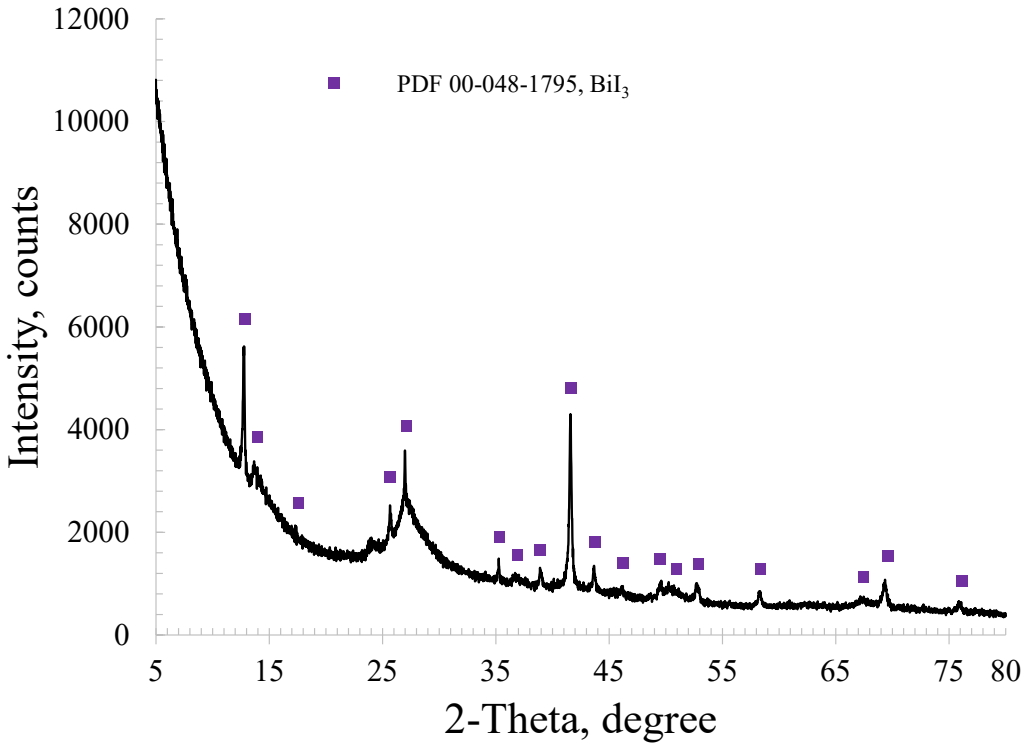

Figure 3. XRD patterns with identified phase for iodine-loaded Bi-aerogel.

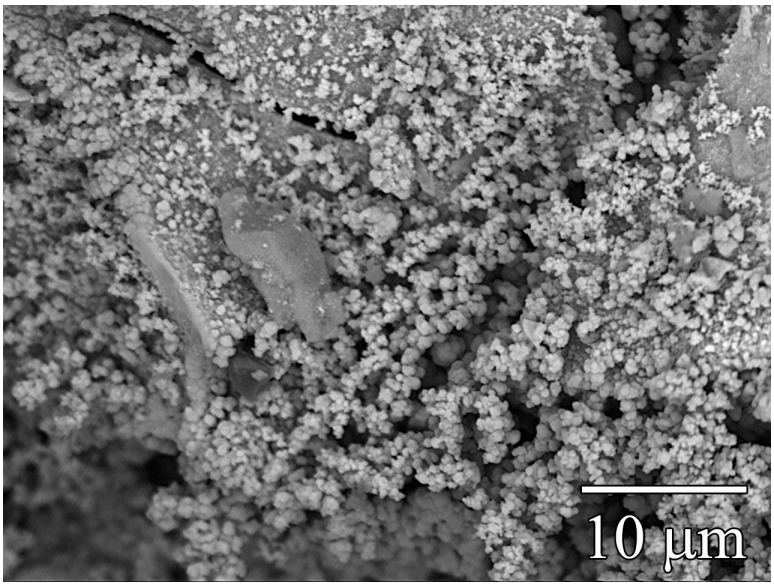

Figure 4. SEM micrograph of Bi^{3+}-aerogel with particles of bismuth oxide nitrate hydroxide hydrate (white features) precipitated on the aerogel support (gray background).

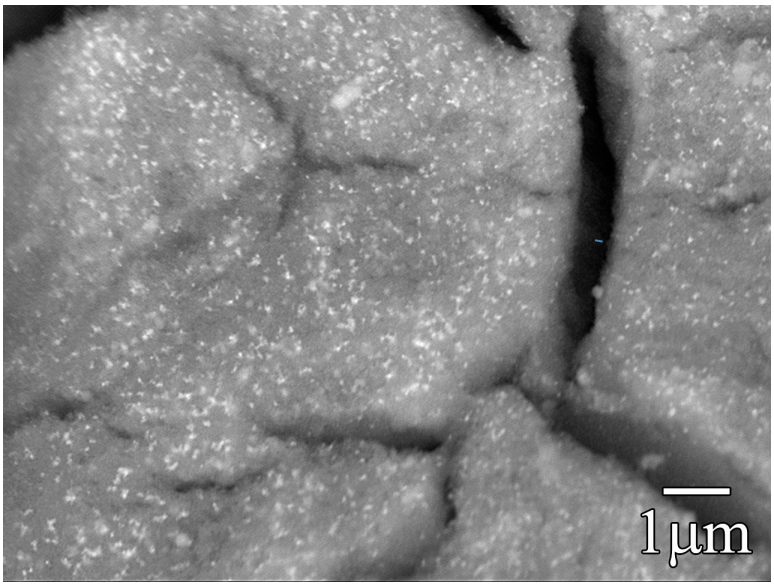

Figure 5. SEM micrograph of Bi-aerogel with nanoparticles of bismuth and bismuth sulfide (white features) formed on silica aerogel support (gray background).

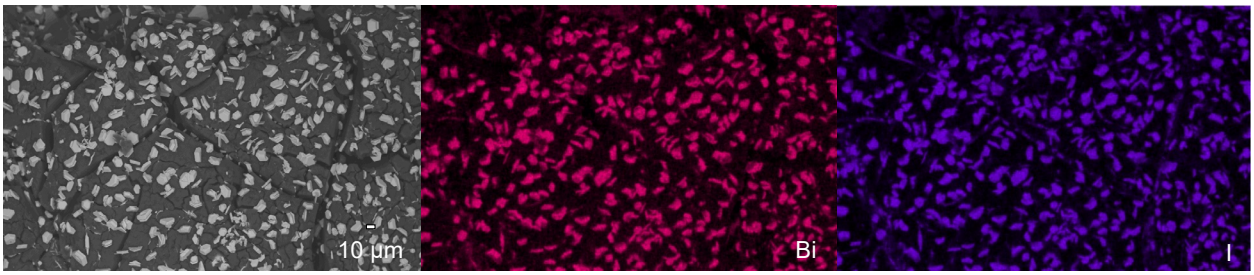

Figure 6. SEM micrograph of bismuth iodide particles for iodine-loaded Bi-aerogel compared with overlay EDS dot maps for Bi and I.

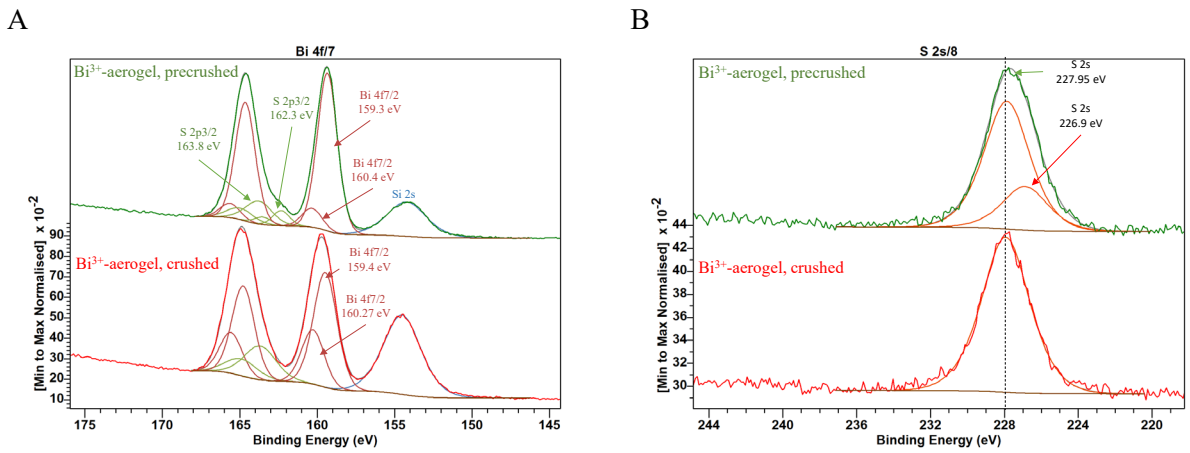

Figure 7. XPS plots for (A) Bi4f/5 and (B) S 2s/6 for pre-crushed and freshly crushed granules of Bi^{3+}-aerogel.

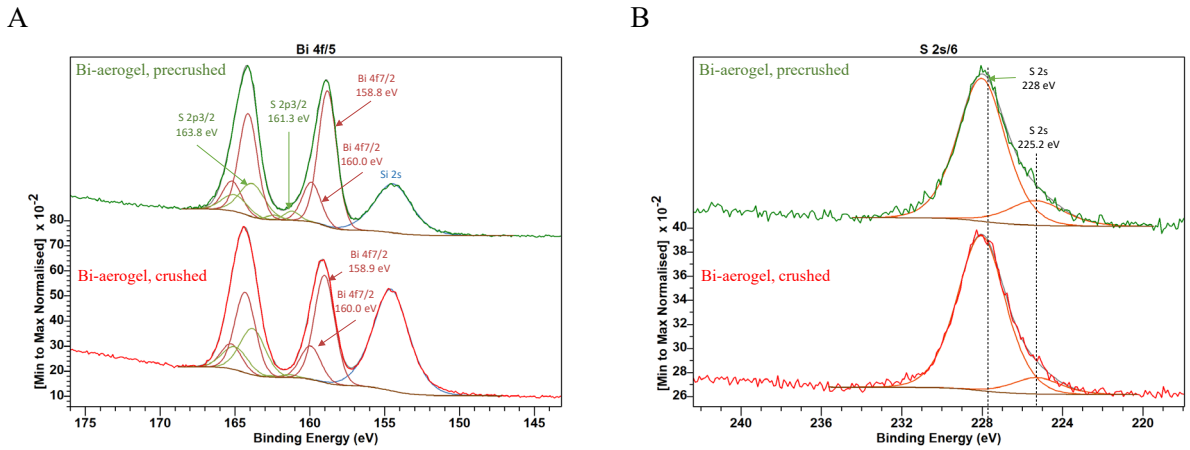

Figure 8. XPS plots for (A) Bi4f/5 and (B) S 2s/6 for pre-crushed and freshly crushed granules of Bi-aerogel.

5 SUMMARY AND CONCLUSIONS

Two types of bismuth-functionalized silica aerogels were successfully manufactured, one with bismuth oxide nitrate hydroxide hydrate particles (Bi^{3+}-aerogel) and another with bismuth metal and bismuth sulfide nanoparticles (Bi-aerogel). Both sorbents exhibited high sorption capacity for iodine. However, the presence of particles of different compositions, sizes, and distributions on aerogel supports resulted in different iodine loadings. The Bi^{3+}-aerogel exhibited sorption capacity of 289 mg/g. In contrast, Bi-aerogel exhibited more that 20% higher sorption capacity. The heat-treatment of Bi^{3+}-aerogel at 225°C under hydrogen atmosphere increased iodine loading capacity to 351 mg/g. This study demonstrated feasibility of bismuth-functionalized silica aerogel for an efficient capture of iodine from off-gas streams also due to environmentally friendly character and low cost of bismuth as compared to silver, the metal traditionally used for these applications.

6 ACKNOWLEDGEMENTS

This work was funded by the U.S. Department of Energy (DOE) Office of Nuclear Energy's Nuclear Technology Research and Development Program. Pacific Northwest National Laboratory is operated for DOE by Battelle Memorial Institute under Contract DE-AC05-76RL01830. The authors greatly appreciate constructive comments and suggestions by Brian Riley from PNNL.

7 REFERENCES

Asmussen, R.M., J.V. Ryan, J. Matyáš, J.V. Crum, J.T. Reiser, N. Avalos, E.M. McElroy, A.R. Lawter, N.C. Canfield, Investigating the Durability of Iodine Waste Forms in Dilute Conditions. *Materials* 2019, *12*, 686. https://doi.org/10.3390/ma12050686.

Bruffey S. H., K. K. Anderson, R. T. Jubin, and J. F. Walker Jr., *Aging and iodine loading of silver-functionalized aerogels*, FCRD-SWF-2012-000256, Oak Ridge National Laboratory, Oak Ridge, Tennessee, 2012.

Bruffey S. H., K. K. Anderson, R. T. Jubin, and J. F. Walker Jr., *Humid Aging and Iodine Loading of Silver Functionalized Aerogels*, FCRD-SWF-2013-000258, Oak Ridge National Laboratory, Oak Ridge, Tennessee, 2013.

Bruffey S. H., K. K. Patton, R. T. Jubin, *Complete Iodine Loading of NO-Aged Ag^0-Functionalized Silica Aerogel*, FCRD-MRWFD-2015-000419, Oak Ridge National Laboratory, Oak Ridge, Tennessee, 2015a.

Bruffey S. H., K. K. Patton, J. F. Walker Jr., R. T. Jubin, *Complete NO and NO_2 Aging Study for AgZ*, FCRD-MRWFD-2015-000631, Oak Ridge National Laboratory, Oak Ridge, Tennessee, 2015b.

Einarsrud M.-A., E. Nilsen, A. Rigacci; G. M. Pajonk, S. Buathier, D. Valette, M. Durant, P. Chevalier, P. Nitz, and F. Ehrburger-Dolle, Strengthening of Silica Gels and Aerogels by Washing and Aging Processes. *Journal of Non−Crystalline Solids*, 285, 1−7, 2001.

Jubin R. T., S. H. Bruffey, and K. K. Patton, *Humid Aging and Iodine Loading of Silver-Functionalized Aerogels*, FCRG-SWF-2014-000594, Oak Ridge National Laboratory, Oak Ridge, TN, 2014.

Jubin R. T., D. Strachan, *Assessments and Options for Removal and Immobilization of Volatile Radionuclides from the Processing of Used Nuclear Fuel*, ORNL-SPR-2015/115, Oak Ridge National Laboratory, Oak Ridge, TN, 2015.

Kramer S. J., F. Rubio-Alonso, and J. D. Mackenzie, "Organically modified silicate aerogels, "Aeromosils", Materials Research Society Symposium Proceedings 435:295–300, 1996.

Matyáš J., G. E. Fryxell, B. J. Busche, K. Wallace, and L. S. Fifield, "Functionalized silica aerogels: Advanced materials to capture and immobilize radioactive iodine," in Ceramic Materials for Energy Applications (Eds. H. Lin, Y. Katoh, K. M. Fox, I. Belharouak, S. Widjaja, and D. Singh), John Wiley & Sons, Inc., Hoboken, New Jersey, US, doi: 10.1002/9781118095386.ch3, *Ceramic Engineering and Science*, 32(9), 23-33, 2011.

Matyáš, J. N. Canfield, S. Sulaiman, and M. Zumhoff, "Silica-based waste form for immobilization of iodine from reprocessing plant off-gas streams," *Journal of Nuclear Materials* 476, 255-261, 2016.

Matyáš, J., G. E. Kroll, and X.S. Li, *Improvement of mechanical stability of Ag^0-functionalized silica aerogel,* FCRD-MRWFD-2018-000214, Pacific Northwest National Laboratory, Richland, 2018.

Matyáš, J., G.R. Kroll, and X. Li., *Mechanically Stable Silver-Functionalized Silica Aerogel*, PNNL-29048. Pacific Northwest National Laboratory, Richland, WA, 2019.

Matyáš, J., S. E. Sannoh, and X. Li., *Development of a Robust Ag^0-Functionalized Silica Aerogel for Capturing Iodine Gas*, PNNL-30732. Pacific Northwest National Laboratory, Richland, WA, 2020.

Matyáš, J., S.E. Sannoh, and X.S. Li., *A preliminary investigation of co-adsorption of other halogens on engineered form of Ag^0-aerogel*, PNNL-31222, Pacific Northwest National Laboratory, Richland, WA, 2021.

Oliver W. C., G. M. Pharr, "Measurement of hardness and elastic modulus by instrument indentation: Advances in understanding and refinements to methodology," *Journal of Materials Research* 19(1), 3-20, 2004.

Soelberg N. and T. Watson, *Iodine Sorbent Performance in FY 2012 Deep Bed Tests*, FCRD-SWF-2012-000278 (INL/EXT-12-27075), Idaho National Laboratory, Idaho Falls, Idaho, 2012.

Tavlarides L.L., Presentation at MRWFD Working Group Meeting in Richland, WA, 27 March 2019.